

**Nonlinear sensors: An approach to the residence time detection strategy**

A. Dari, L. Bosi, and L. Gammitoni\*

*NiPS Laboratory, Dipartimento di Fisica, Università di Perugia, 06100 Perugia, Italy and INFN Sezione di Perugia, 06100 Perugia, Italy*

(Received 17 November 2008; revised manuscript received 2 August 2009; published 12 January 2010)

The monitoring of the residence time difference in bistable sensors has been recently proposed as a valid scheme for improving the detection capabilities of sensors as diverse as fluxgate magnetometers, ferroelectric sensors and mechanical sensors. In this paper we propose an approach to the residence time based detection strategy based on the measurement of the slope  $m$  of the sensor output integral. We demonstrate that such a method, far from degrading the detection performances can provide an easier way to realize fast and reliable sensors without the computationally demanding task related with the computation of the residence time difference. We introduce the receiver operating characteristic curve as a quantitative estimator for the comparison of the two methods and show that the detector performances increase with increasing the periodic bias amplitude  $A$  up to a maximum value. This condition has potentially relevant consequences in the future detectors design.

DOI: [10.1103/PhysRevE.81.011115](https://doi.org/10.1103/PhysRevE.81.011115)

PACS number(s): 05.40.Ca, 07.07.Df

**I. INTRODUCTION**

A considerable number of sensor devices manifest a nonlinear input-output relationship, often in the form of bistable response characteristic. These include magnetic sensors such as fluxgates [1], ferroelectric sensors [2], and mechanical sensors [3], e.g., acoustic transducers, made with piezoelectric materials. The functioning of these devices, for some purposes, can be described in terms of dynamical systems acted on by a combination of deterministic and stochastic inputs. For such systems, it is common to assume a bistable potential energy function  $V(x)$  (although it is not uncommon the case of the so-called *excitable systems* where a threshold discriminates between the two states [4]), where the two stable states, located at the minima  $\pm x_m$  of  $V(x)$ , are separated by an unstable point represented by the maximum of the potential, located at  $x=0$ . The two minima are thus separated by a potential barrier with height  $\Delta V_{\pm} = V(0) - V(\pm x_m)$ . If we assume the system to be symmetric,  $\Delta V_+ = \Delta V_- = \Delta V$ . In this framework, the dynamics of the sensor is usually expressed in terms of the motion of a massive particle in the static potential  $V(x)$ , subjected to some deterministic forces  $A(t)$  representing the signal to be sensed and by a random force  $\xi(t)$  representing the unavoidable noise that affects the sensor functioning.

The presence (detection) and the value (estimation) of the unknown signal  $A(t)$  are assessed through a careful monitoring of the dynamic system output  $x(t)$ . Due to the presence of a nonlinear input-output relationship such monitoring activity is not straightforward and a number of different approaches to the problem have been developed, with specific reference to the peculiarities of the input signal  $A(t)$ . In this paper we will focus on the well known problem of sensing a direct current (dc) or low-frequency signal. This is a classical problem of signal analysis that, in the case of nonlinear (bistable) potential has not yet received a completely satisfy-

ing solution. As an example, conventional fluxgate sensors use a strategy based on the monitoring of the power spectral density amplitude of the second harmonic of the response to a periodic driving bias signal. Be  $A(t) = B(t) + \varepsilon$  the input signal, where  $\varepsilon$  is the dc signal to be sensed and  $B(t) = A \sin(\omega_0 t)$  is an externally added bias periodic signal. The system output  $x(t)$  will still be a periodic signal but due to the nonlinear character of the system, there will be the presence of higher harmonics of the fundamental  $\omega_0$ . In particular, if  $\varepsilon = 0$ , due to the symmetry of the dynamics there will be only even harmonics. The appearance of odd harmonics can thus be associated with the presence of a non-null target signal:  $\varepsilon \neq 0$ . However, such a detection strategy has some drawbacks, mainly related with the computationally demanding task of the estimation of the second harmonic of a given signal.

On the other hand, particularly in the last few years, sensor device miniaturization has become increasingly relevant in order to attain higher level of integration, higher performance and low energy consumption. Continuous downscaling drastically increases the presence of disturbances of various nature that can be collectively addressed as noise affecting the sensing operation. Noise can affect the functioning of sensors in a number of ways, with the final results of limiting its sensitivity.

To circumvent problems due to the traditional strategy and to operate in presence of noise, a readout approach has been proposed using statistics in order to gain information on the presence of small target signals. This approach is based on the monitoring of the mean residence time difference [5–9]. The residence time is the time the system output spends in each of the two stable states. In the presence of the input signal  $A(t)$ , if  $A$  is large enough and if  $\omega_0$  is small enough, the system output  $x(t)$  is a periodic signal with amplitude proportional to  $x_m$  and its dynamics is composed by large excursions between one minima and the other, across the potential barrier. If  $\varepsilon \neq 0$ , the system dynamics  $x(t)$  is markedly asymmetric and the time  $x(t) > 0$  is different from the time  $x(t) < 0$ . If we set two thresholds  $+b$  and  $-b$ , we can define a state transition from the state  $+$  to the state  $-$  when

\*luca.gammitoni@pg.infn.it

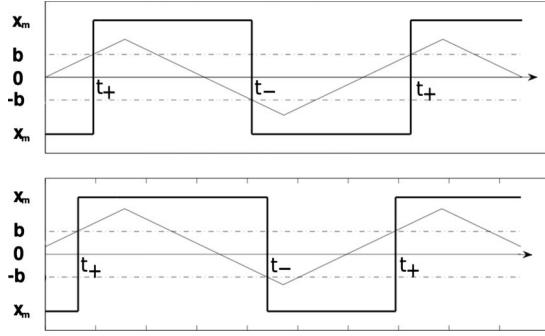


FIG. 1. Schmitt trigger model in the deterministic condition [ $A(t)$  is a triangular wave function with the bias amplitude  $A$  larger than the barrier] for the case where no dc signal is present (upper) and for the case where there is a signal with constant amplitude  $\varepsilon$  (lower). In the two figures the input and the output time series are represented. Apparently, in the upper panel the residence times are equal, while in the lower panel the two residence times are different.

$x(t)$  crosses  $-b$  from above. We say that the system output is in the  $-$  state as long as a  $-$  to  $+$  transition happens, i.e., when  $x(t)$  crosses  $+b$  from below (see Fig. 1).

We are now in position to define the residence time (RT) in the  $+$  state as the time interval  $T^+$  between the instant of a  $-$  to  $+$  state transition and the subsequent instant of the first  $+$  to  $-$  state transition. Analogously we can define  $T^-$  as the time interval between the instant of a  $+$  to  $-$  state transition and the subsequent instant of the first  $-$  to  $+$  state transition. The residence time difference is defined then as  $\Delta T = T^+ - T^-$ . For what we have said, if  $\varepsilon = 0$  and the system dynamics is symmetric then  $\Delta T = 0$ . On the other hand, if  $\varepsilon \neq 0$  then  $\Delta T \neq 0$ . Thus monitoring  $\Delta T$  we can obtain information on the value of the unknown signal  $\varepsilon$ .

The use of residence time as an indicator of the system dynamics was initially proposed in [10]. In fact, in the presence of external noise the RT becomes a random variable whose value changes with each sample. In this case it is customary to consider the mean value of the residence time, i.e.,  $\langle T^+ \rangle$  and  $\langle T^- \rangle$ , respectively. Here  $\langle \dots \rangle$  indicates an average over the statistical ensemble.

Although noise and nonlinearity are usually considered undesirable features of sensors, there are cases where they can be employed in a cooperative way in order to improve the sensitivity. An example is the so-called *stochastic resonance* (SR) phenomenon [11,12]. The notion of SR was originally introduced [13] to describe a property peculiar to bistable systems subjected to a *weak* periodic modulation embedded into a noise background: for a certain value of the noise intensity the fundamental periodic component of the system response gets amplified to an optimal amplitude. Another remarkable effect is the *dithering* effect [14] that finds useful applications in ADC (analog-to-digital converters) and *resonant crossing* [15] effect as well. Taking into account this realistic scenario where nonlinearity and noise are unremovable system characteristics, it has been advanced the idea that a class of sensors can be conceived, the so-called *noise activated nonlinear devices* [5], where noise and nonlinearity can cooperate in order to improve the device functioning.

Starting from the known results of the residence time based detection strategy [5,6], the aim of this paper is to present and discuss a method to simplify the sensor operation. Specifically, we propose to estimate the difference between the mean residence times in the two stable states by computing a quantity,  $I(\tau)$ , represented by the integral over time of the system output. The function  $I(\tau)$  has a definite relationship with the mean residence time difference  $\Delta T$  and results composed by two contributions: one step function and a periodic function. By monitoring the slope of the first integral component, versus time, we can obtain the value of the target signal, instead of measuring the computationally demanding  $\Delta T$ .

The paper is organized as follows: after analyzing the operating conditions and after resuming the main characteristics of the residence time based detection strategy, we present our approach. Initially we show the analytical calculation for the deterministic case and then we investigate the effect of asymmetry in presence of noise. We compare our approach to the standard determination of the residence time difference with respect to the detection capabilities of the two methods. We conclude that the two methods perform equally well and thus our approach has to be preferred because it can be implemented with less computational effort. We also observe that, with reference to the detection task, the detector performances increase with increasing the periodic bias amplitude  $A$  up to a maximum value. I.e., it exists a  $A = \bar{A}$  value for the amplitude above which the detection capability does not increase and remain constant. This has some relevant consequences in the detector design.

## II. RESIDENT TIME-BASED DETECTION STRATEGY

The nonlinear sensors, studied in this paper, work in a noisy environment and only few dynamical variables can be adjusted to improve their performance. Specifically, the ambient noise and the target signal characteristics cannot be modified at will, while the bias signal (amplitude and frequency) and the reference thresholds can be arbitrarily adjusted.

As analyzed in [6], the starting point of the residence time difference detection strategy is the monitoring of the switch dynamics in a symmetric, unperturbed bistable system. In order to fix our ideas, avoiding the complex features of a continuous dynamics, we will consider in the following a two state discrete dynamical model. As in [6] the Schmitt Trigger (ST) model is assumed. Compared to the continuous dynamical model (e.g., the bistable Duffing oscillator), the ST output is completely controlled by the switching mechanism between the two steady states (the interwell motion), while the intrawell dynamic (that is the motion around the potential minima) is neglected. In the following we will consider a ST model characterized by two static barriers at  $\pm b$  with an input signal  $f(t)$  that consists of two components: (i) a noisy signal  $\zeta(t)$  and (ii) a signal to be sensed  $A(t)$ ,

$$f(t) = A(t) + \zeta(t). \quad (1)$$

We assume the noise  $\zeta(t)$  to be Gaussian band limited (exponentially correlated) having zero mean, and correlation

time  $\tau_0$  [5]. The noise  $\zeta(t)$  originates from a white noise driven Ornstein-Uhlenbeck (OU) process:  $\dot{\zeta} = -\lambda_0 \zeta + \sigma F(t)$ , where  $\lambda_0 \equiv \tau_0^{-1}$ , and  $F(t)$  is white noise having zero mean and unitary strength.  $\zeta(t)$  has correlation function  $\langle \zeta(t) \zeta(s) \rangle = \sigma_\zeta^2 \exp[-|t-s|/\tau_0]$  with variance  $\sigma_\zeta^2 = \sigma^2 \tau_0 / 2$ .

The ST output is a dichotomic signal with values  $\pm x_m$ . Being  $x(0) = x_m$ , the system output rests in this state as long as the input  $f(t) < -b$  with  $t > 0$ . As soon as  $f(t)$  crosses  $-b$  the trigger switches (almost) instantaneously into the lower state  $-x_m$  and sits there until  $f(t) < b$ . The deterministic component of  $f(t)$ , i.e.,  $A(t)$ , is usually characterized by a periodic bias signal  $B(t)$ , that can be introduced to control the bistable sensor dynamic and is chosen in the *suprathereshold* regime (i.e., the amplitude of  $B(t)$  is larger than  $b$ ), and by a small unknown dc target signal  $\varepsilon$  ( $\varepsilon \ll b$ ),

$$A(t) = B(t) + \varepsilon, \quad (2)$$

After presenting the hypotheses of the present strategy, we are now ready to discuss its main working principle. Using the ST model we will compute the two residence times,  $T^+$  and  $T^-$ , as defined previously. Considering the presence of noise these two variables have a random nature, thus the so relevant quantities will be replaced by the averaged residence times:  $\langle T^+ \rangle$  and  $\langle T^- \rangle$ , respectively. Accordingly  $\langle \Delta T \rangle = |\langle T^+ \rangle - \langle T^- \rangle|$  and it will be a function of the input signal and will carry the information about the target signal amplitude. In the symmetric case ( $\varepsilon = 0$ ) the two values  $\langle T^+ \rangle$  and  $\langle T^- \rangle$  are identical and the mean residence time difference is zero. For a nonzero target signal,  $\varepsilon \neq 0$ , the input signal is on average closer to one of the thresholds (see Fig. 1) and thus the residence time values in the two states are different. As a consequence  $\langle \Delta T \rangle = |\langle T^+ \rangle - \langle T^- \rangle| > 0$ .

In order to reach a quantitative understanding of the behavior of  $\langle \Delta T \rangle$ , let's consider at first the case where no noise is present. Moreover, by the moment that the role of the specific wave form of the bias signal has been discussed elsewhere [6], for the sake of simplicity we will consider here a triangular signal  $B(t)$  of amplitude  $A$ ,

$$B(\tau) = \begin{cases} 4A(\tau - n) & \text{if } n \leq \tau < n + \frac{1}{4} \\ 2A(1 - 2(\tau - n)) & \text{if } n + \frac{1}{4} \leq \tau < n + \frac{3}{4} \\ 4A(-1 + (\tau - n)) & \text{if } n + \frac{3}{4} \leq \tau < n + 1 \end{cases} \quad (3)$$

with  $\tau = t/T_0$ , where  $T_0$  is the period of the triangular wave and  $n = \text{int}(\tau)$ , which means the integer part of  $\tau$ .

To obtain the value of the residence time difference in this condition, we compare  $A(t) = B(t) + \varepsilon$  with the two thresholds  $\pm b$ . The relevant crossing times  $\tau_+$  and  $\tau_-$  in the absence of noise are readily computed as

$$\tau_+ = \frac{b - \varepsilon}{4A}, \quad (4)$$

$$\tau_- = \frac{b + \varepsilon}{4A} + \frac{1}{2}, \quad (5)$$

The crossing times refers, respectively, to the instant of the first upward crossing of the upper threshold (lower-to-upper state switch) and to the instant of the first downward crossing of the lower threshold (upper-to-lower state switch), i.e.,  $\tau_+ = t_+/T_0$  and  $\tau_- = t_-/T_0$ . Taking into account the input signal defined in Eq. (3), the ST output assumes the  $\pm x_m$  values at the considered crossing times,

$$x(\tau) = \begin{cases} -x_m & \text{if } n \leq \tau < \tau_+ + n \\ x_m & \text{if } \tau_+ + n \leq \tau < \tau_- + n \\ -x_m & \text{if } \tau_- + n \leq \tau < n + 1, \end{cases} \quad (6)$$

To obtain the  $\Delta T$  it is necessary to monitor the switches between the two states by keeping track of the chronology of each crossing. In a single period,  $T^+ = t_- - t_+$  and  $T^- = T_0 - T^+$ ,

$$T^+ = T_0(\tau_- - \tau_+) = T_0 \left( \frac{A + \varepsilon}{2A} \right), \quad (7)$$

$$T^- = T_0[1 - (\tau_- - \tau_+)] = T_0 \left( \frac{A - \varepsilon}{2A} \right). \quad (8)$$

Finally, we obtain

$$\Delta T = |2T^+ - T_0| = T_0 \frac{\varepsilon}{A}. \quad (9)$$

As it is well apparent, there is a linear dependence between the residence time difference and the target signal amplitude: a quite desirable condition in a sensor [15].

### III. INTEGRAL DETECTOR

The measurement of the mean residence time difference in a real bistable device is a quite troublesome goal to reach. As detailed in the previous section, the  $\Delta T$  is obtained by monitoring the chronological crossings. In fact,  $T^+$  and  $T^-$  have to be computed from the switching times and, after accumulating such quantities, mediated to finally generate  $\langle \Delta T \rangle = |\langle T^+ \rangle - \langle T^- \rangle|$ .

This strategy has been implemented to achieve a sensor with higher sensitivity and a simplified procedure compared to the traditional method. However, the computation of the mean residence time difference can be quite demanding, especially in the case where a stand-alone microsensor is involved. Fortunately, as we are going to show, such a direct computation can be avoided, without giving up with the residence time approach.

Let us consider the following quantity:

$$I(\tau) = \int_0^\tau x(s) ds. \quad (10)$$

In a single period  $t = T_0$  and thus  $\tau = 1$ ; we have:

$$I(1) = \int_0^1 x(s)ds = \int_0^{\tau_+} x(s)ds + \int_{\tau_+}^{\tau_-} x(s)ds + \int_{\tau_-}^1 x(s)ds. \tag{11}$$

By substituting the values for  $\tau_+$  and  $\tau_-$  and considering the system output  $x(t) = \pm x_m$  we can easily obtain

$$I(1) = x_m[2(\tau_- - \tau_+) - 1] = x_m \frac{\varepsilon}{A}. \tag{12}$$

For a generalization to a generic instant of time, we assume  $\tau > 0$  and we compute the value of the integral. This consists of two contributions: a step function (that increases every period  $T_0$  by a quantity proportional to  $\varepsilon$ ) and a triangular function that superimposes onto the step function,

$$I(\tau) = X_{\text{step}}(\tau) + X_{\text{tri}}(\tau), \tag{13}$$

with

$$X_{\text{step}}(\tau) = nx_m \frac{\varepsilon}{A}, \tag{14}$$

where  $n = \text{int}(\tau)$ , and

$$X_{\text{tri}}(\tau) = x_m \begin{cases} -\tau & \text{if } n \leq \tau(\tau_+ + n) \\ (\tau - 2\tau_+) & \text{if } \tau_+ + n \leq \tau(\tau_- + n) \\ 2(\tau_- - \tau_+) - \tau & \text{if } \tau_- + n \leq \tau(n + 1). \end{cases} \tag{15}$$

If we consider  $I(\tau_i)$ , where  $\tau_i = i + \tau(0)$  and  $i = 0, 1, \dots$ , it is easy to realize that these values lies in a straight line. For different  $\tau(0)$  we have different straight lines that have the same slope, but different starting point. The slope of these lines is readily identified as

$$m = x_m \frac{\varepsilon}{A}. \tag{16}$$

Based on these results we are now in position to present a detection strategy for the measurement of  $\varepsilon$ : in order to gain information on the target signal  $\varepsilon$  it is sufficient to measure the slope of the straight line obtained by sampling the output integral  $I(t)$  at regular intervals, each spaced by an integer multiple of the period  $T_0$ . Quite conveniently, also in this case the measured quantity is proportional to  $\varepsilon$ . We stress the fact that this approach allows us to circumvent the difficulties connected to the direct  $\Delta T$  computation that is usually performed with a digital signal processing (DSP) system. On the other hand the measurement of the quantity just introduced can be performed both with a DSP and also, most importantly, with analog electronics by means of a running average on the signal. This can be realized with a low pass filter, RC type. This second solution is by far less demanding both by the electronic complexity point of view and by the energetic demand point of view. Two points, these that are quite relevant in the autonomous sensors design.

#### IV. IN THE PRESENCE OF NOISE

The previous theoretic calculation has been restricted to the deterministic case. However, in order to obtain a more

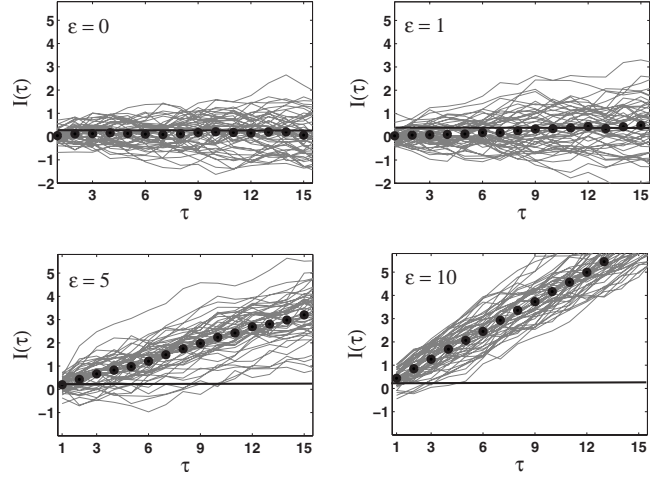


FIG. 2.  $I(\tau)$  versus  $\tau$ , with  $\tau = t/T_0$ , for four different values of the target signal  $\varepsilon$ . With dots we have plotted the average value  $\langle I(\tau) \rangle$ . These values are used to compute the linear regression and to extract  $\langle m \rangle$ .

realistic description, it is mandatory to take into account the role of noise, unavoidably present in each measurement. In this section we will discuss the possibility of implementing the *slope-based* measurement strategy, in the presence of external additive noise. In the following we assume that  $f(t) = A(t) + \zeta(t)$ , where the noise  $\zeta(t)$  statistical properties have been defined above. Because of the noise, the slope  $m$  computed from different time series, behaves here as random variable. The relevant quantity will thus be assumed to be its ensemble average  $\langle m \rangle$ . In order to study the behavior of  $\langle m \rangle$  as a function of the relevant parameters we realized a digital simulation of the ST dynamics. A number of digital time series of the input and output signal were produced and the statistical average of the relevant quantities computed from these (see e.g., Fig. 2).

We started our investigation by studying the dependence of  $\langle m \rangle$  on the noise intensity for various values of  $A$  ( $\varepsilon = 1$ ).

The results of the digital simulation have been plotted in Fig. 3. A number of features are evident:

- (1) In the so-called *suprathreshold* case, i.e., when  $A > b$

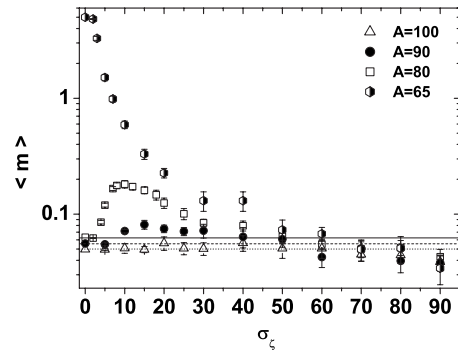


FIG. 3. Slope  $\langle m \rangle$  versus the noise standard deviation  $\sigma_\zeta$ , for four different values of the bias signal amplitude  $A$  with the same frequency  $\nu_0 = 1/T_0$ .  $b = 70$ ,  $\varepsilon = 1$ ,  $T_0 = 5$ , and  $\tau_0 = 0.5$ . The horizontal lines represent the theoretical prediction for the zero noise limit in the suprathreshold case.

+ $\varepsilon$  the dynamics is mainly driven by the deterministic periodic bias  $A(t)$ . Specifically,

(i) For weak noise intensities ( $\sigma_\zeta \ll A - b - \varepsilon$ ) the dynamic is completely driven by the triangular signal amplitude and the obtained  $\langle m \rangle$  value can be approximated by the deterministic calculation. For  $\sigma_\zeta = 0$ ,  $\langle m \rangle = m$  and coincides with the value predicted in Eq. (16): see horizontal lines in Fig. 3.

(ii) Increasing  $\sigma_\zeta$ , the system reaches an intermediate condition:  $\sigma_\zeta \approx A - b - \varepsilon$ . The presence of the right amount of noise induces a failure mechanism in switches of the system between the two stable states. It means that the system will spend a larger time in the two wells increasing the slope value to a maximum [16], an effect known in the literature as *resonant trapping* [17]. The amplitude of this effect and the position of the maximum are clearly a function of  $A$  [18]. It is interesting to note that, as reported in the literature for the  $\Delta T$  behavior [5], the *resonant trapping* mechanism is visible also for  $\langle m \rangle$  and the  $\sigma_\zeta$  value where  $\langle m \rangle$  reaches a maximum, increases with increasing  $A$ .

(2) In the so called *subthreshold* case, i.e., when  $A < b + \varepsilon$ , the role of the noise is determinant in leading the switch mechanism.

(i) When the noise is small ( $\sigma_\zeta \ll b - A - \varepsilon$ ) there are just few rare switches and in the zero noise limit the ST is not able to switch anymore. The system output is thus confined permanently in one of the states. In this case (open star symbols in Fig. 3) the zero noise limit for  $\langle m \rangle = m$  and can be easily computed analytically as

$$I = \int_0^{nT_0} x_m dt = x_m n T_0, \quad (17)$$

and thus:

$$m = I/n = x_m T_0, \quad (18)$$

that is in good agreement with the value in Fig. 3 for  $A=65$  and  $\sigma=0$ .

(ii) When the noise increases from  $\sigma=0$  the switch probability grows from null to a finite amount. As a result an increasing number of switches take place and the residence time difference decreases, lowering the average slope  $\langle m \rangle$  of the integral.

(3) In the limit of  $\sigma_\zeta \gg A - b - \varepsilon$ , regardless the value of  $A$ , the noise has the main role on the dynamics. The presence of the antisymmetrizing signal  $\varepsilon$  becomes progressively less important and the dynamics becomes more and more symmetric. The value of the slope  $\langle m \rangle$  decreases to zero. In fact, if noise is very large the ST switches frequently between the two stable attractors and the details of the bias signal wave form become decreasingly relevant.

To further characterize the  $\langle m \rangle$  parameter, we simulated the dynamic of the ST varying the bias signal amplitude at a given noise standard deviation and bias frequency. In Fig. 4 we show the behavior of  $\langle m \rangle$  versus  $A$ .

As it is evident the curves present a monotonic decrease toward zero, moving from a value at  $A=0$  that can be estimated by using the computation of the *mean first passage time* [16] for a purely noise driven switch process. Here  $\langle \tau_+ \rangle$  is the average normalized time that the system spends in the

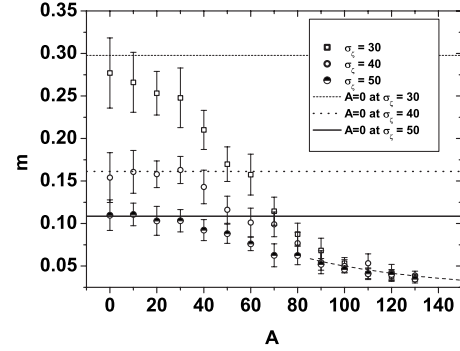


FIG. 4. Slope  $\langle m \rangle$  versus the amplitude  $A$  of the triangular forcing bias for three fixed values of the noise standard deviation  $\sigma_\zeta$ . The horizontal lines represent the theoretical prediction (*mean first passage time*) for the case where only noise is present ( $A=0$ , i.e., zero bias signal amplitude limit). The dashed line is the theoretical prediction for the deterministic limit. The relevant parameters value  $b$ ,  $\varepsilon$ ,  $T_0$ , and  $\tau_0$  are as in Fig. 3.

“+” state, i.e., the average normalized time that the process  $\zeta$  takes to reach the  $-b + \varepsilon$  level, provided that at  $t=0$  was  $\zeta = b + \varepsilon$  and that there is an absorbing boundary in  $-b + \varepsilon$  and a reflecting boundary in  $+\infty$ . Analogously we can define  $\langle \tau_- \rangle$  as the average normalized time that the system spends in the “-” state, i.e., the average normalized time that the process  $\zeta$  takes to reach the  $b + \varepsilon$  level, provided that at  $t=0$  was  $\zeta = -b + \varepsilon$  and that there is an absorbing boundary in  $b + \varepsilon$  and a reflecting boundary in  $-\infty$ .

In these conditions, the value of the integral can be easily expressed in terms of

$$I(\tau_+ + \tau_-) = m(\langle \tau_+ \rangle + \langle \tau_- \rangle), \quad (19)$$

where  $m$  is the slope.

On the other hand we have

$$I(\tau_+ + \tau_-) = \int_0^{\langle \tau_+ \rangle + \langle \tau_- \rangle} x_m dt, \quad (20)$$

$$= \int_0^{\langle \tau_+ \rangle} x_m dt - \int_{\langle \tau_+ \rangle}^{\langle \tau_+ \rangle + \langle \tau_- \rangle} x_m dt, \quad (21)$$

$$= x_m (\langle \tau_+ \rangle - \langle \tau_- \rangle), \quad (22)$$

thus we obtain:

$$m = x_m \frac{\langle \tau_+ \rangle - \langle \tau_- \rangle}{\langle \tau_+ \rangle + \langle \tau_- \rangle}. \quad (23)$$

The horizontal lines in Fig. 4 present our prediction in Eq. (23), in good agreement with the results of the digital simulation.

In the large  $A$  case, i.e., when  $A \gg b + \varepsilon$  the switching mechanism is dominated by the deterministic bias and Eq. (16) holds true:  $m$  is inversely proportional to the bias amplitude (see dotted line in Fig. 4).

We notice here that the highest value of  $m$  is realized when  $A=0$ . Such a condition seems to suggest that the best operating condition for our bistable sensor is one where there

is no periodic bias. This special case is intriguing; it opens up the possibility of operating the sensor with minimal onboard power. However, although it is true that when  $A=0$ ,  $m$  is maximum, by a practical point of view this operating condition has some disadvantages related to the averaging procedure. As a matter of fact, the measure of  $m$  requires an integration procedure carried on in time. If  $m$  is small compared to the noise there might be necessary to carry on a long integration before being able to discriminate between the  $\varepsilon = 0$  and  $\varepsilon \neq 0$  cases. Moreover, a larger  $m$  does not imply, by itself, a higher capability of measuring the target signal. In order to better understand the role of  $A$  in the framework of the proper detection task, in the following section we will address the detection problem more extensively.

## V. DETECTION THEORY

The purpose of a sensor is to measure a physical quantity, by converting it into a suitable signal that can be read by an observer or by an instrument. Because sensor is a real device working in a real world, it has to take into account unavoidable noise sources. There are many different noise sources, some of them can be intrinsic in the device functioning or due to external process such as the environmental working condition.

Noise affects the measurement procedures and causes statistical fluctuations. Due to the unpredictable character of the noise, the possibility to make decisions on the presence or not of a specific target signal is questioned. Due to this, each time a decision about uncertain events has to be taken, it is necessary to follow a statistical approach. Such an attitude has been codified in what is nowadays called “detection theory.” The detection theory provides methods, named “detection strategies,” aimed at maximizing the detection probability and, at the same time, at minimizing the probability of error.

In the following we present some signal detection theory tools that will be useful to assess detection probabilities for our sensor.

### A. Detection strategies

The aim of this section is to provide basic tools of the detection theory. We consider the particular case, relevant here, of a dc signal of amplitude  $\varepsilon$ , embedded into a zero mean white Gaussian noise. Let’s suppose that we have acquired a set of data, represented here by the sequence  $x[n]$ , where  $n=0, 1, \dots, N-1$ . We consider two hypotheses:

$$\begin{aligned} H_0: x[n] &= w[n], \\ H_1: x[n] &= \varepsilon + w[n]. \end{aligned} \quad (24)$$

The first hypothesis is called *null hypothesis* and represents the case when only noise (the sequence  $w[n]$ ) is present in the data. The second hypothesis is called *alternative hypothesis* and in this example represents the case where the data account for a signal composed by noise and the dc term. The detection strategy is aimed at finding a method to declare if

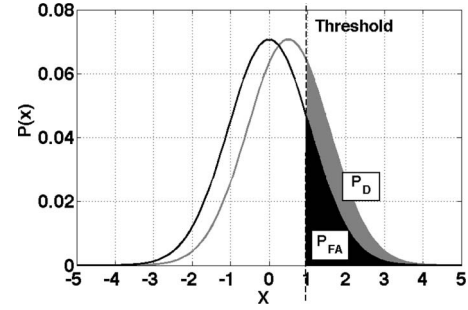


FIG. 5. Probability density for  $x[n]$  and  $\varepsilon=0.5$  under  $H_0$  and  $H_1$ .

the signal  $\varepsilon$  is present or not in the  $x[n]$  data set, thus deciding between the  $H_0$  and  $H_1$  hypothesis.

In Fig. 5 the two distributions for  $x[n]$  and  $\varepsilon=0.5$ , under  $H_0$  and  $H_1$  hypothesis are shown. In the absence of signal ( $H_0$ ) we expect pure noise  $w[n]$  with  $\langle x[n] \rangle = 0$ . On the other hand, under the  $H_1$  hypothesis, we expect a similar distribution, with the same standard deviation but translated for a quantity  $\langle x[n] \rangle = \varepsilon$ . Thus, if on observing the data  $x[n]$ , we find  $x[0] > 1$ , this implies that the observed sample more likely belongs to a distribution with  $\langle x[n] \rangle > 0$  and thus it suggests that more likely  $H_1$  is true. In fact from Fig. 5 is evident how the probability is higher if this value is due to  $H_1$  than to  $H_0$ , i.e.,  $p(x[0]; H_1) > p(x[0]; H_0)$ . Such a probability is named “*detection probability*.” In this way we have built a first naive detector, where we compare an observed datum with a reference value, usually called “*threshold*.”

Following the previous reasoning it is evident that in this procedure two types of errors can be identified. The first error is the *missed detection*, i.e., when we decide for  $H_0$  but  $H_1$  holds instead; the second error is the *false alarm*, i.e., when we decide for  $H_1$  but  $H_0$  holds instead.

We are interested in computing the probabilities of such errors. The probability of false alarm is the probability to claim a signal in the data when there isn’t any. Given the threshold  $\gamma$ , we can write

$$P_{FA} = \int_{\gamma}^{\infty} \frac{1}{2\pi} \exp\left(-\frac{1}{2}t^2\right) dt. \quad (25)$$

In a similar way the probability of detection is the probability to claim the presence of a target signal  $\varepsilon$  in the data when there is one. This is given by

$$P_D = \int_{\gamma}^{\infty} \frac{1}{2\pi} \exp\left(-\frac{1}{2}(t-\varepsilon)^2\right) dt. \quad (26)$$

Where the distribution is by hypothesis Gaussian with a standard deviation equal to 1.

### B. Detection of a dc level in white Gaussian noise

Intuitively, increasing  $\varepsilon$  we expect a better detection due to higher signal. If we consider the previous statistical description, such effect is associable with a better separation between the two Gaussian distributions in Fig. 5.

Under  $H_0$  the  $x[n]$  is a statistical variable with PDF given by

$$p(x;H_0) = \frac{1}{(2\pi\sigma^2)^{N/2}} \exp\left[-\frac{1}{2\sigma^2} \sum_{n=0}^{N-1} x^2[n]\right],$$

while under the  $H_1$  hypothesis we have the same distribution but shifted by  $\varepsilon$ ,

$$p(x;H_1) = \frac{1}{(2\pi\sigma^2)^{N/2}} \exp\left[-\frac{1}{2\sigma^2} \sum_{n=0}^{N-1} (x[n] - \varepsilon)^2\right].$$

Following the Neyman-Pearson theorem [19], we define likelihood ratio as the ratio between two probabilities,

$$L(x) = \frac{p(x;H_1)}{p(x;H_0)}, \quad (27)$$

and we *decide*  $H_1$  if  $L(x)$  is higher of a certain threshold

$$L(x) > \gamma \quad (28)$$

with this definition we have

$$P_{FA} = \int_{x:L(x)>\gamma} p(x;H_0) dx.$$

It is possible to demonstrate [19] that under proper hypothesis the 29 can be reduced to

$$\frac{1}{N} \sum_{n=0}^{N-1} x[n] > \gamma', \quad (29)$$

where  $\gamma'$  is a normalized threshold that includes all the constants and well know parameters of the problem.

In our case,

$$\gamma' = \frac{\sigma^2}{N\varepsilon} \log \gamma + \frac{\varepsilon}{2}. \quad (30)$$

We have now what is called a *Neyman-Pearson detector* based on the comparison of the mean  $\langle x \rangle = \frac{1}{N} \sum_{n=0}^{N-1} x[n]$  to a threshold  $\gamma'$ .

The detection problem can now be addressed with the following steps:

(1) define the problem  $H_0$  and  $H_1$  and its statistical functions  $P_{FA}$  and  $P_D$ ;

(2) calculate the likelihood ratio function;

(3) select the maximum  $P_{FA}$  that is acceptable (this is the arbitrary part of the detection procedure, where we agree on the maximum error rate we can tolerate. For example we can select a  $P_{FA}=10^{-2}$ );

(4) given the  $P_{FA}$  we derive the needed threshold inverting the Eq. (25);

(5) apply the Eq. (28) on data and look if the returned value is higher or lower  $\gamma'$ ;

(6) decide signal  $\varepsilon$  is present if the value is higher than the threshold, vice versa decide that the data are composed only by noise; and

(7) for long data set the procedure is repeated from step 5, dividing data in several overlapping time slices and applying the procedure on each segment.

It is clear how, given the detector, the first critical step is the threshold definition and hence the selection of the acceptable probability of false alarm. This probability is clearly

interlinked with the probability of detection, meaning that we cannot reduce the probability of error (*false alarm* and *missed detection*) by keeping fixed the probability of detection.

In fact, if we try to reduce the  $P_{FA}$ , we need to increase the threshold value. When the threshold is increased the probability to observe output due to noise fluctuation increases, because we are considering now more data from the tail of the Gaussian distribution. But it is also true that we are reducing the probability ( $P_D$ ) to observe outputs due to signal with lower energy.

More in general the decision of the threshold to use is made considering together the  $P_{FA}$  and  $P_D$ . These are linked by [19]

$$P_D = Q\left(Q^{-1}(P_{FA}) - \sqrt{\frac{N\varepsilon^2}{\sigma^2}}\right), \quad (31)$$

where  $Q(\dots)$  is the complementary cumulative distribution [18].

For a fixed  $P_{FA}$  the  $P_D$  increases monotonically with

$$\frac{N\varepsilon^2}{\sigma^2} = R_\delta. \quad (32)$$

This quantity is usually called *signal-to-noise ratio* (SNR) and plays an important role in the detection task. In fact the SNR is proportional to the energy of the signal contained in the data and inversely proportionally to the noise floor.

A relevant indicator of the detector performance is the plot of curves  $P_D$  vs  $P_{FA}$  at different thresholds. These curves are called *receiving operative characteristic* (ROC) curves. Using these plots it is possible, once selected the threshold, to estimate the subsequent expected  $P_{FA}$  and  $P_D$ . Moreover, the ROC curves are often useful to compare different detectors.

### C. Detection strategies for the optimal detector

In the first part of this section we describe the detection strategy of the residence time detector, under the very favorable hypothesis that all the relevant detector parameters are known.

Let's suppose that our data set is

$$x(t) = A \sin(\omega_0 t) + \xi(t) + \varepsilon,$$

where  $A \sin(\omega_0 t)$  is a known periodic signal,  $\xi(t)$  is an exponentially correlated Gaussian noise with zero mean and  $\varepsilon$  is the target dc signal.

The first difference between this problem and the one treated in the previous chapter is the presence of the periodic signal and the exponentially correlated noise. The periodic component is not a problem if it is known, while the correlation of the noise change more deeply the physics of the process and hence the results of the NP detector strategy.

#### 1. NP detector for $\delta$ -correlated noise

Let us consider first the case where there is the periodic signal but the noise is white (i.e.,  $\delta$  correlated). For the delta

correlated case we can demonstrate that the optimal detector is still given by Eq. (29),

$$\frac{1}{N} \sum_{n=0}^{N-1} y[n] > \gamma,$$

where  $y[n]=x[n]-A \sin(\omega_0 n \delta t)$ , with  $\delta t$  the sampling time for the  $y[n]$  time series.

**2. NP detector for exponentially correlated noise**

Here  $\xi(t)$  is an exponentially correlated Gaussian noise with covariance matrix  $C$  and correlation time  $\tau_0 > 0$ . The covariance matrix is defined here as

$$[C]_{mn} = E(\xi[m]\xi[n]) = r_{\xi\xi}[m-n] = \sigma^2 e^{-|m-n|\delta t/\tau_0}.$$

It is possible to demonstrate that the general expression for the NP detector [19] is

$$T(x) = x^T C^{-1} s > \gamma,$$

where  $x$  is the input data vector and  $s$  is the vector containing the signal to be detected, in our case:  $s = \varepsilon \times [1]$  and  $[1]$  is a unit vector.

In order to evaluate the detector performances we introduce the *deflection coefficient*,

$$d^2 = s C^{-1} s,$$

for exponentially correlated noise we have [19]

$$d^2 = \left( \frac{-\frac{n-1}{n} + e^{1/\lambda}}{1 + e^{1/\lambda}} \right) \left( \frac{n\varepsilon^2}{\sigma^2} \right).$$

Where  $\lambda = \tau_0/dt$  with  $dt$  sampling interval.

It is customary to use a large numbers of samples ( $n \gg 1$ ), thus the term  $\frac{n-1}{n}$  can be approximated to 1

$$d^2 = \left( \frac{e^{1/\lambda} - 1}{e^{1/\lambda} + 1} \right) R_{\delta},$$

we have

$$d^2 = \Lambda R_{\delta}.$$

Now we are in position to compare the detector performances in the two cases addressed above:  $\delta$ -correlated noise and exponential-correlated noise. We can observe how the coefficient  $\Lambda \leq 1$ , showing how the effect of the noise exponential correlation is to reduce the detection probability respect to the  $\delta$ -correlated case.

The effect of a finite correlation time on the ROC is shown in Fig. 6 where we compare three pairs of curves with SNR equal to 6, 10, and 20. As it is well apparent for every fixed  $P_{FA}$  the corresponding  $P_D$  of the  $\delta$ -correlated noise outperforms the  $P_D$  of the exponentially correlated noise.

**D. Detection strategies for the suboptimal detector**

In the previous sections we have presented the detection strategies for the case where the data set is given by

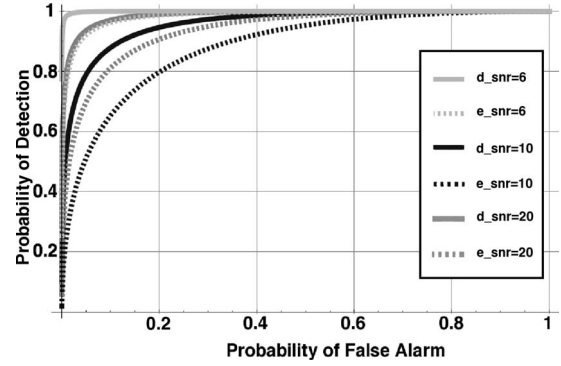


FIG. 6. ROC curves for the two cases:  $\delta$ -correlated noise (continuous line) and exponentially correlated noise (dashed line) for three values of the SNR: 6, 10, and 20. Here  $\lambda = 1$  for all the curves.

$$x[n] = A \sin(\omega_0 n \delta t) + \xi(n \delta t) + \varepsilon.$$

In the most general case the data set is a nonlinear function of this expression. Such a complication is introduced by the sensor employed to sense and transduce the physical signal into a data set ready to be processed by a proper detector. Moreover, for a generically complex data set it is not always possible to identify an optimal detector and thus one is often faced with the problem of employing a suboptimal detection strategy [20]. In these cases a numerical approach to the computation of the ROCs under NP-strategy approach is required. This is clearly the case of the residence time detector and integral detector introduced above. Specifically we are interested in evaluating the ROCs for the two detectors and compare them.

**E. ROCs comparison**

Hence the two detector described in Sec. II are suboptimal. Both the residence time detector and the integral detector are quite simple detectors and members of the energy detectors family. These detectors generically are aimed at extracting the signal energy, by suppressing the stochastic part of the signal via averaging procedures. For the sake of comparison, in Fig. 6 we show the ROC of the optimal detector together with the ROC for the integral detector. As we expected, the integral detector is outperformed by the optimal detector.

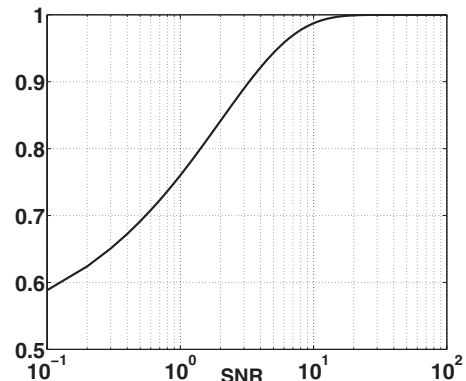


FIG. 7. ROC area versus SNR for the  $\delta$ -correlated case.



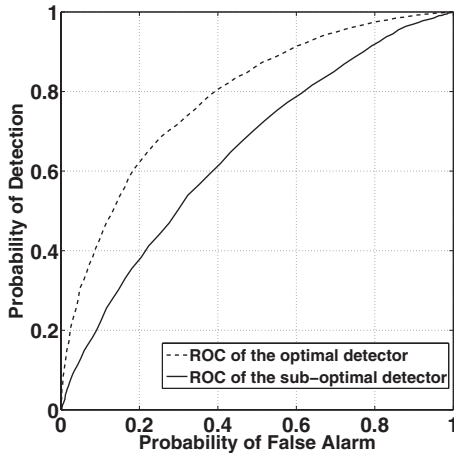


FIG. 8. ROC of the optimal detector compared with the ROC for the Integral Detector (dotted lines). Here  $\varepsilon=1$ ,  $\sigma=10$ ,  $b=70$ ,  $A=100$ , and  $\omega_0=0.2$ .  $\langle m \rangle$  is computed from a time series of  $T=60$  averaged  $10^4$  times.

In the following we focus our attention to the comparison of the integral detector with the residence time detector performances.

In order to simplify the analysis we introduce the concept of ROC area that can be demonstrated to be correlated with the detection performance of a detector for a given SNR. In particular, if we consider fixed the SNR of the physical process, different detectors will recover different amounts of energy and produce different ROCs. As it is well apparent in Fig. 7 we observe that a better detection is associated to a curve with higher area value. Under the optimal hypothesis of NP detector for dc signal in Gaussian white noise case, the relation between ROC area and SNR is shown in Fig. 8. In this case the ROC area is a monotone function of the SNR. In all cases the ROC area has a lower bound at 0.5 and higher bound at 1.

With respect to the optimal case, we expect for the sub-optimal detectors and for a given SNR, a lower ROC area value. Hence, ROC area is a good parameter, useful for the detectors performance comparison, where the higher bound is represented by the area of the optimal detector.

In Fig. 9 we show the difference between the ROC area computed for the  $\Delta T$  observable and for the  $m$  observable. As it is well apparent the difference is in the range of few

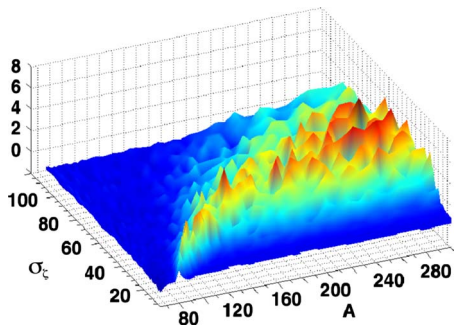


FIG. 9. (Color online) ROC area percentage difference versus the amplitude  $A$  of the periodic force for different values of the noise intensity  $\sigma$ . The other parameter values are  $\varepsilon=1$  and  $b=70$ .

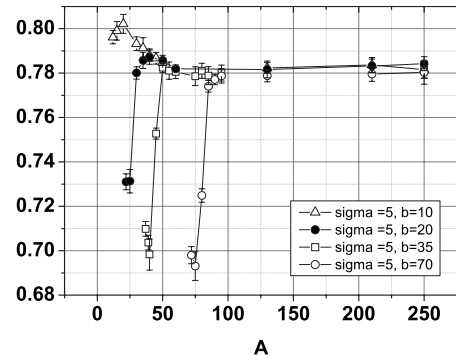


FIG. 10. ROC area for  $\langle m \rangle$  versus the amplitude  $A$  of the periodic force for different values of the noise intensity  $\sigma$ . The other parameter values are  $\varepsilon=1$ ,  $b=70$ , and  $\omega_0=0.2$ .  $\langle m \rangle$  is computed from a time series of  $T=60$  averaged  $10^4$  times.

percent and well within the statistical fluctuation of the two quantities. These results support our proposal of using the observable  $m$  instead of  $\Delta T$ . In fact the two quantities are statistically equivalent from the point of view of the detection performances and thus, in principle,  $m$  should be preferred due to the easier way to compute this quantity.

In these two detectors four parameters  $A$ ,  $\varepsilon$ ,  $\sigma$ , and  $b$  are defined. Not all the parameters are independent. Specifically we can rescale amplitudes by introducing the ratio between one parameter and the others. Thus if we want to characterize the detectors performances we need to cover a three-dimensional space parameters.

In Fig. 10 we present the ROC area versus the amplitude  $A$  of the periodic force. As is apparent it does exist a  $\bar{A}$  value above which the area does not increase anymore. Such a value scales with  $\sigma$  and  $b$  apparently according to  $\bar{A} \approx b+2\sigma$ . Moreover for large  $A$  the values of the ROC area for various  $\sigma$  and  $b$  converges approximately to the same asymptotic value. It is also worth noting that on decreasing  $b$  the curve develops a maximum before converging to the large  $A$  plateau.

In Fig. 11 we present a more general perspective of the ROC area versus both the amplitude  $A$  of the periodic force and the noise intensity  $\sigma$ . As previously observed, once the noise intensity is fixed, for  $A > \bar{A}$  the ROC area does not increase anymore (Fig. 12). Moreover the  $\bar{A}$  increases with increasing  $\sigma$ . This has some relevant consequences in the detector design. In fact, as we noticed at the end of Sec. IV with reference to Fig. 4, the highest value of  $m$  is realized when  $A=0$ . However such a condition that can be relevant in order to operate the sensor with the highest sensitivity does not coincide with the best detector operating condition. Such a condition, for what it is apparent in Fig. 10 is reached instead for  $A \approx \bar{A}$ . At the same time Fig. 10 suggest that there is no advantage in using a larger  $A$ , i.e.,  $A > \bar{A}$ .

VI. CONCLUSIONS

In this paper we have analyzed the performances of an approach to the residence time based detection strategy. Such

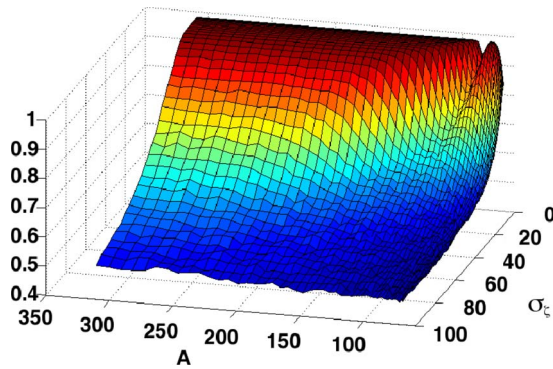


FIG. 11. (Color online) ROC area for  $\langle \Delta T \rangle$  versus the amplitude  $A$  and  $\sigma_c$ . The other parameter values are  $\varepsilon=1$ ,  $b=70$ , and  $\omega_0=2.0$ .  $\langle \Delta T \rangle$  is computed from a time series of  $T=120$  averaged 5000 times.

an approach, based on the measurement of the slope  $m$  of the sensor output integral, is shown to perform equally well with the standard method based on the measurement of the mean residence time difference  $\Delta T$ . Thanks to the easier way to implement the method this has to be preferred to the standard one. We have computed the ROC area as a quantitative estimator of the detector performances and observed that the detector performances increase with increasing the periodic

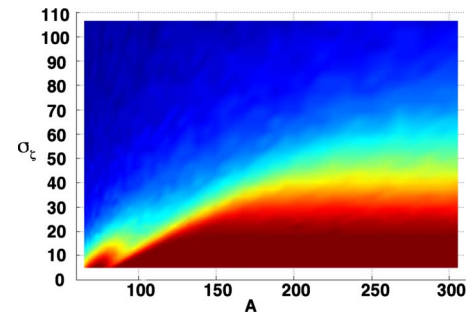


FIG. 12. (Color online) ROC area versus the amplitude  $A$  and  $\sigma_c$ . The same parameter values as in Fig. 11.

bias amplitude  $A$  up to a maximum value. This amount to say that it exists a  $A=\bar{A}$  value for the amplitude above which the detection capability does not increases and remains constant. This condition has potentially relevant consequences in the detector design.

#### ACKNOWLEDGMENT

The authors gratefully acknowledge financial support from European Commission (FPVI, STREP Contract No. 034236, Sub KT Low Energy Transistors and Sensors).

- 
- [1] P. Ripka, *Sens. Actuators, A* **106**, 8 (2003).  
 [2] I. Bunget and M. Prohescu, *Physics of Solid Dielectrics* (Elsevier, New York, 1984).  
 [3] J. Fraden, *Handbook of Modern Sensors, and References Therein* (AIP Press, New York, 1997).  
 [4] M. Cizak, M. Camarda, F. Marino, F. Marin, and A. Ortolan, *Phys. Rev. D* **76**, 103001 (2007).  
 [5] L. Gammaitoni and A. R. Bulsara, *Phys. Rev. Lett.* **88**, 230601 (2002).  
 [6] A. R. Bulsara, C. Seberino, L. Gammaitoni, M. F. Karlsson, B. Lundqvist, and J. W. C. Robinson, *Phys. Rev. E* **67**, 016120 (2003).  
 [7] L. Gammaitoni and A. Bulsara, *Physica A* **325**, 152 (2003).  
 [8] B. Andò, S. Baglio, A. R. Bulsara, and V. Sacco *Measurement* **38**, 89 (2005).  
 [9] A. Nikitin, N. G. Stocks, and A. R. Bulsara, *Phys. Rev. E* **68**, 036133 (2003).  
 [10] L. Gammaitoni, F. Marchesoni, E. Menichella-Saetta, and S. Santucci, *Phys. Rev. Lett.* **62**, 349 (1989).  
 [11] L. Gammaitoni, P. Hänggi, P. Jung, and F. Marchesoni, *Rev. Mod. Phys.* **70**, 223 (1998).  
 [12] F. Marchesoni, L. Gammaitoni, F. Apostolico, and S. Santucci, *Phys. Rev. E* **62**, 146 (2000).  
 [13] R. Benzi, G. Parisi, A. Sutera, and A. Vulpiani, *Tellus* **34**, 10 (1982).  
 [14] L. Gammaitoni, *Phys. Rev. E* **52**, 4691 (1995).  
 [15] L. Gammaitoni, F. Marchesoni, E. Menichella-Saetta, and S. Santucci, *Phys. Rev. Lett.* **71**, 3625 (1993).  
 [16] A. Dari and L. Gammaitoni, *Model and Design of Complex Systems* (Springer, Berlin, 2009), p. 225.  
 [17] F. Marchesoni, F. Apostolico, L. Gammaitoni, and S. Santucci, *Phys. Rev. E* **58**, 7079 (1998).  
 [18] F. Apostolico, L. Gammaitoni, F. Marchesoni, and S. Santucci, *Phys. Rev. E* **55**, 36 (1997).  
 [19] S. M. Kay, *Detection Theory* (Prentice Hall, Englewood Cliffs, NJ, 1998), Vol. 2.  
 [20] M. E. Inchiosa and A. R. Bulsara, *Phys. Rev. E* **53**, R2021 (1996); V. Galdi, V. Pierro, and I. M. Pinto, *ibid.* **57**, 6470 (1998); M. E. Inchiosa and A. R. Bulsara, *ibid.* **58**, 115 (1998); M. E. Inchiosa, A. R. Bulsara, and L. Gammaitoni, *ibid.* **55**, 4049 (1997).